Biomechanical Property Quantification of Prostate Cancer by Quasi-static MR Elastography at 7 Telsa of Radical Prostatectomy, and Correlation with Whole Mount Histology

D. M. McGrath[1], W. D. Foltz[1], N. Samavati[1], J. Lee[1], M. A. Jewett[2], T. H. van der Kwast[3], C. Ménard[1], and K. K. Brock[1,4]

[1]Radiation Medicine Program, Princess Margaret Hospital, Toronto, Ontario, Canada, [2]Department of Surgical Oncology, Princess Margaret Hospital, Toronto, Ontario, Canada, [3]Department of Pathology, University Health Network, Toronto, Ontario, Canada, [4]Department of Radiation Oncology, University of Toronto, Toronto, Ontario, Canada

INTRODUCTION Magnetic resonance elastography (MRE) is a powerful tool for the detection and localization of cancer, as has been well demonstrated in organs such as liver (1) and breast (2). Application to the prostate is in development (3), and holds enormous potential for MRI-guided prostate intervention for cancer, such as targeted radiation therapy, MRI-guided biopsy or high dose rate (HDR) brachytherapy (4). MRE parameters could potentially replace or complement currently used MRI parameters for prostate cancer localization, i.e., T_2-weighted (T2w) signal, apparent diffusion coefficient (ADC), dynamic contrast enhanced MRI (DCE-MRI) parameters (5) and MR spectroscopic imaging (MRSI) (6). To inform development, quantitative data on the relative increase in biomechanical stiffness of prostate cancer above that of normal tissue is required. Some initial work using ex vivo tissue has been carried out using dynamic MRE (7). However, these methods are hampered by poor spatial resolution, difficulties in achieving uniform mechanical wave excitation across the sample, and dependency of the results on the wave frequency. To obtain high spatial resolution quantitative data of the whole prostate, an initial investigation has been made applying a quasi-static MRE method at high magnetic field strength (7 tesla) to radical prostatectomy tissue, for which the disease burden was assessed via whole-mount histopathology. Correlation was determined of the MRE-measured tissue stiffness with histopathology-identified disease, and with prostate anatomical structure. MRE was also used to measure the increase in tissue stiffness caused by pathology processing in fixative solution.

METHODS A whole prostate specimen was received from a patient with biopsy-confirmed reoccurrence of cancer in the peripheral zone, after earlier treatment with targeted radiation therapy. The tissue (~4 cm diameter) was embedded in a cube (7×7×7 cm^3) of gel prior to imaging (8). The quasi-static MRE method (8) employed a compression device consisting of a sample holder, a compression plate and mechanical piston, connected via an eccentric disk to a non-magnetic ultrasonic piezo-electric motor (USR60-E3N, Shinsei, Japan), providing compression at 1 Hz with maximum amplitude of 1.5 mm. The device was placed in the bore of a 7-T pre-clinical MRI scanner (70/30 BioSpec, Bruker, Ettlingen, Germany), where a quadrature volume resonator (15.5 cm inner diameter) was used for transmission and reception. A Stimulated Echo (STEAM) sequence (8) was used, with a gradient duration τ = 1 ms and amplitude Gd = 40 mT/m, and therefore a displacement sensitivity ϕ_d of 3.4π/mm. The mixing time T_m between the 2nd and 3rd STEAM 90° pulses was 200 ms and TR = 1s. Acquisitions were made of 23 slices of 3 mm thickness, with 0.5×0.5 mm^2 in-plane resolution (160×160 matrix), in a slice plane approximately perpendicular to the axis of the urethra. Echo planar (EPI) readout was used: TE = 16 ms, NEX = 7, segments = 17, requiring ~1 hr for the total acquisition. To assist the correlation of MRI with histopathology, a high resolution 3D T2w RARE (Rapid Acquisition with Relaxation Enhancement) acquisition was also made, with isotropic voxel dimensions = 0.3×0.3×0.3 mm^3 (matrix=233×233×233), TE=8.5 ms, TR=2400 ms, echo train length=16. On scan completion the sample was removed from the gel and submersed in 10% neutral buffered formalin for pathology fixation over a period of ~60 h. The fixed sample was re-embedded in gel and the MRE scan repeated. Next the specimen was sectioned at 3 mm slice thickness in a cutting plane approximately perpendicular to the axis of the urethra. The sections were processed for whole mount histology to produce one slide per section, and each was stained with Hematoxylin and Eosin (H&E). The pathology-identified tumor regions were marked on the slides, which were digitized on a TISSUEscope™ 4000 (BiomedicalPhotometrics Inc., ON, Canada). The 3D T2w MRI volume was digitally resampled at varying axial oblique slice angles (using in-house software developed in Matlab, The MathWorks, Natick, MA) to find the best match of anatomical structure in the MRI slices to that in the histopathology slices. Quantitative maps of Young's Modulus (*E*) for each MRE imaging slice were calculated (8) and these maps were also resampled digitally to the best match angle. The histology images were manually translated and rotated in-plane (using Matlab) to provide the best match of anatomical structure and position to the MRE signal image slices (pre-fixation data). The tumor areas defined by histology were used to select disease regions on the co-registered MRE-maps. Also, the regions corresponding to stiffer muscular tissue were manually segmented on the MRE maps. The four central slices of the prostate were selected for analysis, as the bulk of the disease was present in this location, with tumors extending through > 3 mm (i.e., slice thickness). Normalized histograms of *E* were calculated and compared for the following tissue subsets: 1) prostate excluding the stiffer muscular tissue and histology-defined tumor; 2) muscular tissue; 3) histology-defined tumor. To explore the use of MRE to define tumor regions, a lower threshold for *E* was applied to the MRE maps (excluding the muscular tissue regions). The threshold was varied over a range (0-500 kPa) to determine the value that maximized the Dice-similarity index of the MRE-defined tumor areas and the histology-defined tumor areas.

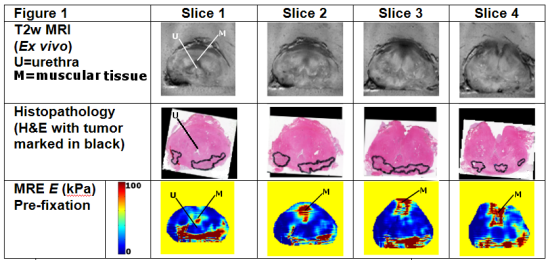

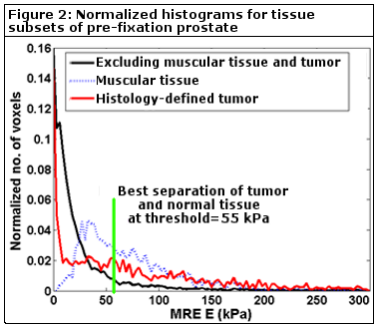

RESULTS The T2w MRI, histology images and MRE *E* maps of the four central slices are displayed in Figure 1. To verify disease margins, segments of attached extra-prostatic tissue were excised with the prostate (see T2w images); these areas were masked out of the MRE *E* maps. Pathology identified adenocarcinoma, which was found predominantly in the peripheral zone. Only some portions of disease are discernable as low T2w signal in the peripheral zone; however all tumors have corresponding areas of increase in MRE *E* (although T2w contrast for disease is likely to be reduced post radiation therapy). Table 1 provides summary data for MRE. The mean *E* of pre-fixation prostate (excluding muscular tissue and tumor) of 37 kPa corresponds with ~36 kPa (12 kPa Shear modulus) reported for normal prostate in (7). Tumor areas defined by histology were significantly stiffer (3-fold, p<0.0001, 2-sample t-test) than the region excluding tumor and muscular tissue. However, the muscular tissue was also significantly stiffer (2-fold, p<0.0001). The comparison of histograms (Figure 2) indicates that muscular tissue should be neglected if MRE is used to automatically identify disease. Furthermore, the highest Dice-similarity index (0.4) occurred at a threshold of 55 kPa, which agrees with a threshold of ~54 kPa (18 kPa Shear modulus) identified by (7). The Gleason scores ranged 7-9, however no correlation was measured with *E*. Fixation caused an 8-fold increase in mean *E* for the four slices. Figure 3 shows an example post-fixation *E* map (corresponding to pre-fixation slice 4) showing increased stiffness in a non-uniform pattern.

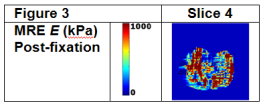

Table 1	Tissue subset	MRE *E* (kPa)	
		Mean (±Std)	Median
Pre-fixation	Excluding muscular tissue and histology- defined tumor	37(± 90)	14
	Muscular tissue	72(± 47)	61
	Histology-defined tumor	111(± 163)	60
Post-fixation	All tissue	612(±805)	344

DISCUSSION AND CONCLUSION Quasi-static MRE at 7 T provides fine spatial resolution coverage of the entire sample and demonstrates sensitivity to disease. Furthermore, it reveals the variability of stiffness in normal prostate; information not obtained using dynamic MRE. This data could inform a strategy for MRE-guided tumor detection. Although this sample was obtained post radiation treatment, the glandular tissue stiffness is comparable to non-irradiated tissue values. The increase in stiffness with fixation demonstrates how measurements for disease should be made pre-fixation, and this data will be used to inform biomechanical model based registration strategies for improved correlation of histopathology with imaging (8). The technique will be applied to further prostatectomy specimens to allow calculation of population-wise data.

REFERENCES 1. Venkatesh SK et al, *Amer J Roent* 2008;190:1534-1540; 2. McKnight AL et al, *Amer J Roent* 2002;178:1411-1417; 3. Sinkus R et al, Proc Intl Soc Mag Res Med 2003;11:586; 4. Ménard C et al, *Int J Radiation Oncology Biol Phys* 2004;59(5):1414-1423; 5. Langer DL et al, *Radiology* 2010;255(2):485-494; 6. Pucar D et al, *Radiology* 2005;236(2):545-553; 7.Dresner M, et al, *Proc. ISMRM* 2003 p.578; 8. McGrath DM et al, *Proc. ISMRM* 2010 p.640